Nonminimum Phase Behavior of Laser Material Processing

G.R.B.E. Römer[1], N.P. Weerkamp[1], J. Meijer[1] and S. Postma[2]

[1]*University of Twente, Faculty of Engineering, Enschede, The Netherlands,*
g.r.b.e.romer@ctw.utwente.nl
[2]*Netherlands Institute for Metals Research, Delft, The Netherlands*
s.postma@ctw.utwente.nl

Abstract

Optical sensors are increasingly applied in laser material processing to monitor and control the laser-material interaction zone. Dynamic models, relating the sensor signals (e.g. as temperature or molten area) to the process inputs (e.g. laser power or beam velocity), provide the basis for the design and tuning of a feedback controller. These models can show nonminimum phase (NMP) behavior. This means that the sensor signal of a minimum phase process directly changes in the direction of its steady-state value, whereas the sensor signal of the NMP process is initially in the opposite direction. This paper illustrates and discusses the NMP behavior found in three different laser processes. Firstly, the behavior is shown theoretically for laser heating, using a Finite Element Model (FEM). Here the beam velocity is used as an input and the temperature (as well as molten area) is the model output. Secondly, the NMP behavior is shown experimentally for laser alloying of titanium. In this case again the beam velocity is applied as input, whereas a pyrometer signal is considered as output. Finally, laser welding of mild steel is discussed. Here the laser power is considered as input, and the intensity of the plasma radiation as output. Whether or not a process shows NMP behavior is essential information in the design and tuning of model based feedback controllers.

1. Introduction

The time response $y(t)$ of a process (dynamic system) to an input $u(t)$ can be modelled in the frequency domain by a linear (or can be approximated by a linear) *transfer function* $H(s)$ (see figure 1)

$$H(s)=\frac{y(s)}{u(s)}=\frac{a_m s^m + a_{m-1}s^{m-1} + \cdots + a_1 s + a_0}{b_n s^n + b_{n-1}s^{n-1} + \cdots + b_1 s + b_0},\ n \geq m \qquad (1)$$

in which $s=j\omega$ denotes the complex frequency, with $\omega=2\pi f$ and f the frequency in Hz, and where $y(s)$ and $u(s)$ denote the Laplace transforms of the time domain output $y(t)$ and input $u(t)$ signal respectively[1].

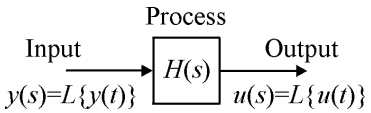

Figure 1: The input-output relation of a dynamic system (process) is described by its transfer function H(s). Here L{·} denotes the Laplace transform.

In the case of laser material processing, the laser power $P(t)$ or the beam velocity $v(t)$ could be considered as input signals. Whereas, for example, the light emitted by the plasma plume during welding, or the thermal radiation (temperature) of the melt pool, captured by an optical detector (photodiode) can be considered as an output signal $y(t)$.

The roots of the denominator polynomial (i.e. those values of s for which the denominator polynomial equals zero), in expression (1) are referred to as the *poles* of the dynamic system, and are denoted by p_i, $i \in \{1,\dots n\}$. Hence, a process has n (real valued or complex) poles, where n is referred to as the order of the process. The poles of stable processes, like laser material processing, have negative real parts–i.e. $\forall\ p_i$, $i \in \{1,\dots n\}$ have $\mathrm{Re}(p_i)<0$. The values of the poles are related to the time constant(s) of the dynamic system.

The roots of the numerator polynomial are referred to as the *zeros* z_j, $j \in \{1,\dots m\}$. A dynamic system is said to be a *nonminimum phase* (NMP) system if one, or more, of its zeros have positive real parts, –i.e. $\exists\ z_j$, $j \in \{1,\dots m\}$ with $\mathrm{Re}(z_j)>0$. The name NMP is derived from the frequency response of such a system[1]. However, the difference between a minimum phase process and a NMP process can be best illustrated by their response to a step-like change of the input signal $u(t)$, see figure 2a.

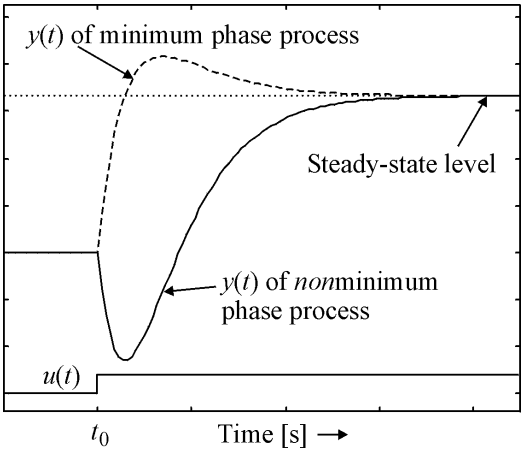

(a) Time response of a minimum phase and a NMP process to a step-like change of the input signal u(t) at $t=t_0$.

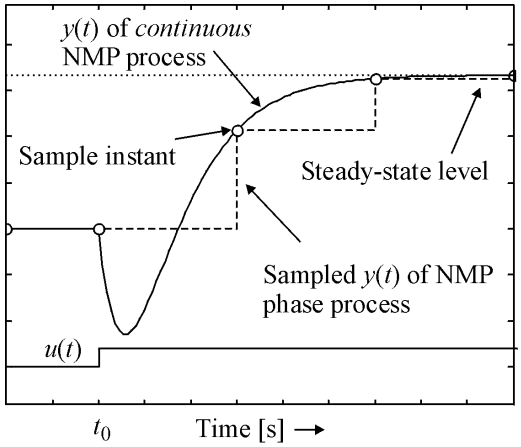

(b) If the sample period h [s] is long compared to the dynamics of the process, NMP behavior will not be visible in the sampled output y(t).

Figure 2: Time-response response of (non)minimum phase processes.

After the change of the input signal at $t=t_0$, the output of a minimum phase process directly changes in the direction of its steady-state value, whereas the response of the NMP process is initially in the opposite direction.

So far, only continuous time process (models) have been discussed. Computers are increasingly used to sample the sensor signals (output $y(t)$ of the process) at a fixed sample period h [s]. In that case, the corresponding discrete-time transfer function $G(q^{-1})$

$$G(q^{-1}) = \frac{y(k)}{u(k)} = \frac{a_m q^{-m} + a_{m-1} q^{-m+1} + \cdots + a_1 q^{-1} + a_0}{b_n q^{-n} + b_{n-1} q^{-n+1} + \cdots + b_1 q^{-1} + b_0},\ n \geq m \qquad (2)$$

relates the k-th output sample $y(k)$ to the k-th input sample $u(k)$, and where q^{-1} denotes the backward shift operator. The model parameters (a, b, n and m) of such a discrete time transfer function can either be calculated from the continuous time transfer function[2], or directly from the sampled signals by system identification (see section 3). A discrete-time process shows NMP behavior, if one or more of its zeros z_j,are positive and outside the unit disc, i.e. if $\exists\ z_j$, with $\mathrm{Re}(z_j)>1$.

It is important to note that, if the sample period h is (chosen too) long, compared to the time constants of the process, the NMP behavior of a continuous NMP process may be concealed in the sampled signal and thus in the discrete-time model, see figure 2b. As today's computers and sensors are sufficiently fast (short sample period), NMP behavior may be found in laser material processing.

At first, it may be surprising that thermal processes (like laser material processing) can exhibit NMP behavior. After all, one would expect that decreasing the laser power (or increasing the beam velocity) will result directly in lower temperatures, a smaller melt pool, or a less intense plasma radiation (and vise versa). And not, as in NMP process, initially a decrease of these quantities, before increasing to their steady-state values. In the following three sections, NMP behavior will be shown in heat diffusion (laser heating), laser alloying and laser welding.

2 Heating

A two dimensional heat flow in a solid work piece (plate), induced by a moving line heat source, was modeled by a Finite Element Model (FEM) and simulated using the software package ANSYS[3]. This model was used to simulate and analyze the time-response of the temperature distribution of the plate, due to changes in the beam velocity v. It approximates the temperature distribution, at some distance from (but not in, or close to) the melt pool, during full penetration welding of plates. The heat flow is described by the heat conduction equation

$$\rho c_p \frac{\partial T}{\partial t} = \nabla \cdot \lambda \nabla T + Q \qquad (3)$$

in which T [K] denotes the temperature at a location (x,y) at time t in the plate. As a material the titanium alloy Ti6Al4V was considered, which is characterized by a density of ρ=4428 $\mathrm{kg \cdot m^{-3}}$, a specific heat of c_p=564 $\mathrm{J \cdot (kg \cdot K)^{-1}}$ and a heat conductivity of λ=6.8 $\mathrm{W \cdot (m \cdot K)^{-1}}$. The absorbed laser energy of the moving laser beam (line heat source) is accounted for by the time dependent source term $Q(v,t)$. The appropriate boundary conditions were applied–i.e. no heat flow over the edges and surfaces of the plates, except for the flow of laser energy.

To solve this partial differential equation, the ANSYS' FEM element *PLANE55* was used on a grid of 81×121 nodes, with dimensions of 50µm and 125µm per element in x and y direction respectively, see figure 3. The element is defined by four nodes, each with the temperature as the single degree of freedom. The temperature distribution over the element is defined by linear interpolation. The absorbed laser energy (here 100W), is distributed over 4 adjoining elements, when positioned on a node, as shown in figure 3. It is assumed that the energy is completely absorbed in the 1mm thick plate. Hence, $Q=100/(1\cdot 10^{-3}\cdot \Delta x \cdot \Delta y)=1.6\cdot 10^{13}$ [W/m^3]. This corresponds to a uniform energy distribution over one element. As the temperature distribution is known to be symmetric with respect to the y-axis (see figure 5), only half of de work piece was simulated (see figure 3) to save computation time. This is achieved by setting $\partial T/\partial x=0$ at $x=0$, as

a boundary condition. Correspondingly, also half of the load is applied Q=0.8·10^{13} [W/m^3], distributed over 2 adjoining elements.

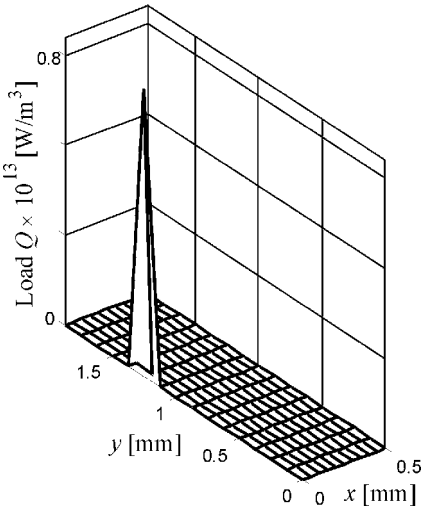

Figure 3: Part of the FEM grid and its load distribution (power density of absorbed laser power)

The time step of the simulation was set at Δt=1.5ms, which guarantees computational convergence. The beam velocity was set at 40mm/s. The steady-state solution (t approaches infinity) of the temperature distribution was found to match with the analytical solution of Rosenthal[4].

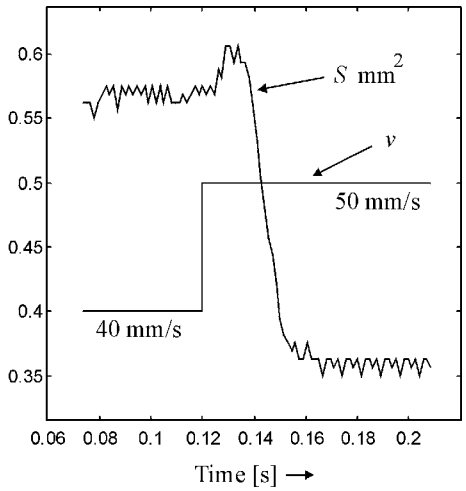

(a) Area of the temperature distribution above 905 °C, within a circular FOV of 3mm.

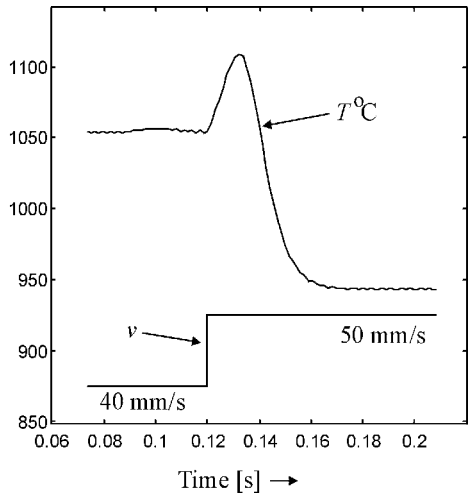

(b)Temperature at 1mm behind the center of the laser spot.

Figure 4: NMP behavior of the laser heating process.

To demonstrate the NMP behavior of laser heating, the beam velocity (input in figure 1) was changed step-wise from 40 to 50 mm/s at t=0.12s. As the output of the process was considered, the number of nodes showing a temperature larger than 905°C, and which are confined within a

circle with diameter d_{FOV}=3mm, centered around the laser beam. This output corresponds to an (optical) sensor with a Field Of View (FOV) of 3mm, measuring the area of the temperature distribution above 905°C. Figure 4a, shows this "area" S (number of nodes multiplied by $dA=\Delta x\cdot\Delta y$), as a function of time. The high frequency variations in the results are rounding errors. It is clear from the figure that this model (and thus the process) shows NMP behavior. That is, due to the increase of beam velocity at t=0.12s, initially the area S increases from $S\approx0.55\text{mm}^2$ to $S\approx0.6\text{mm}^2$, before decreasing to its stead-state value 0.35mm^2 at $t\approx0.17$s. Also the temperature just behind the center of the laser spot (output $y(t)$ in figure 1) shows NMP behavior when the beam velocity (input in figure 1) is changed step-wise, see figure 4b.

The NMP behavior can be explained from the difference between the beam velocity and the speed of heat diffusion into the material, expressed by the Peclet number[6]

$$\text{Pe}=\frac{v\cdot d_{FOV}}{\kappa}\ [-] \qquad (4)$$

where $\kappa=K/(\rho c_p)$ $[\text{m}^2\cdot\text{s}^{-1}]$ denotes the heat diffusitivity of the material. If the Peclet number is large, as is the case here, the beam velocity is fast compared to the heat diffusion. Hence, when the laser spot is accelerated from 40 to 50mm/s the laser beam will heat additional cold material, whereas the heat of temperature distribution established so far has not (yet) been diffused into the material, to match the new beam velocity. This temporarily results in a larger (mainly longer[6]) temperature distribution at the surface of the sample, see figure 5. Hence, in a temporarily increase of the area S and also of the temperature behind the laser spot.

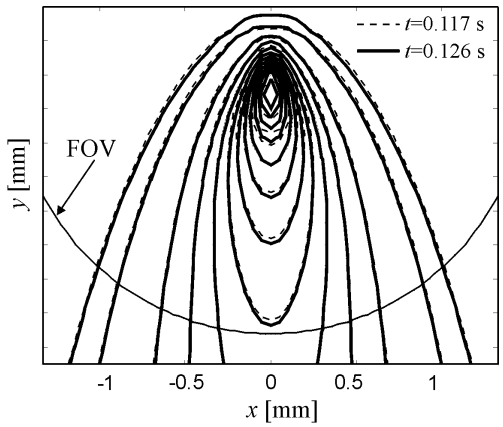

Figure 5: Isotherms at the surface just before and after acceleration of the beam.

It was found that the NMP behavior diminishes when the beam velocity is small compared to the speed of heat diffusion, which is clear from equation (4). The NMP behavior of the area S also diminishes when the FOV of the sensor d_{FOV} is small compared to the dimensions of the temperature distribution. Or when the reference temperature 905°C is decreased or increased significantly. The latter corresponds to a decrease of the FOV.

In the next section the conclusions from this section will be experimentally verified by area and temperature measurements during laser alloying of titanium.

3.Laser alloying of Ti6Al4V

When titanium is melted in a nitrogen atmosphere, extremely hard alloy titanium-nitride (TiN) is formed[5]. A ROFIN SINAR CO_2-laser source (TEM_{01}*+TEM_{00}), with measured power rise time of 22μs, and a spot diameter at the surface of the work piece of d=1.1mm, was applied, see figure 6a. The Ti6Al4V work piece (∅40 by 4mm) was sandblasted and mounted on an XY-table. Nitrogen gas was supplied through a tube from aside. A thermographic CCD camera (128×128 pixels, peak sensitivity at approximately 950nm) was used to monitor the melt pool[6]. In addition, two pyrometers were applied to monitor the process: a KLEIBER spectral pyrometer (975nm, rise time 0.3ms) and an IMPAC ratio pyrometer (950nm & 1050 nm, spot size ∅0.45mm, rise time 10ms). The FOVs of the sensors were aligned as shown in figure 6b. That is, the FOV of the spectral pyrometer is centered around the melt pool, whereas the FOV of the ratio pyrometer is positioned about 1 mm behind the center of the laser spot.

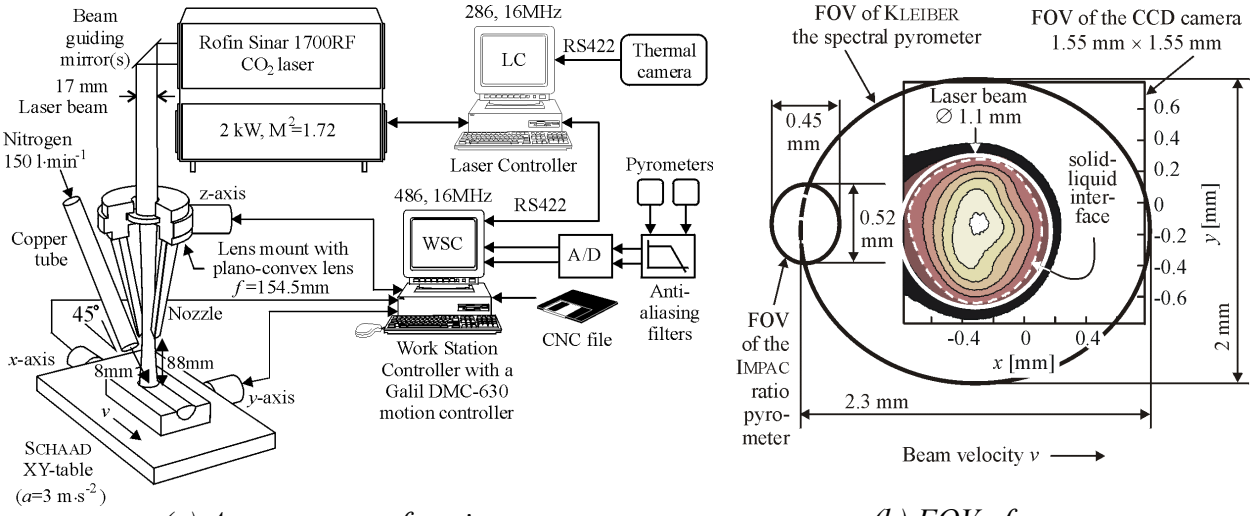

(a) Arrangement of equipment *(b) FOV of sensors*

Figure 6: Experimental setup of laser alloying of Ti6Al4V

It can be shown that variations in the signal of the spectral pyrometer are mainly determined by variations in the area of the melt pool and to a lesser extend due to variations in the melt pool temperature[7]. Therefore, this signal is denoted by $S_{m,T}$ [°C]. The signal of the ratio pyrometer is denoted by T_i [°C]. During the experiment the laser power was varied between 1150 and 1350W, whereas the beam velocity was varied between 40 and 60 mm/s, see figure 7a. The NMP behavior of this process is not directly clear from this experiment. Therefore, system identification was used to derive a dynamic model of the process, relating the inputs (laser power and the beam velocity) to the outputs (signals of the two pyrometers). Hence, a MIMO (Multiple Inputs Multiple Outputs) model was obtained. System identification is an iterative algorithm, in which the parameters (a_i, b_j and orders n, m) of the transfer function (2) are estimated, such that the model output (predicted pyrometer signals) fit well as possible with the measured inputs (P and v) and outputs (signals of the 2 pyrometers). MATLAB's system identification toolbox was used for these calculations[8].

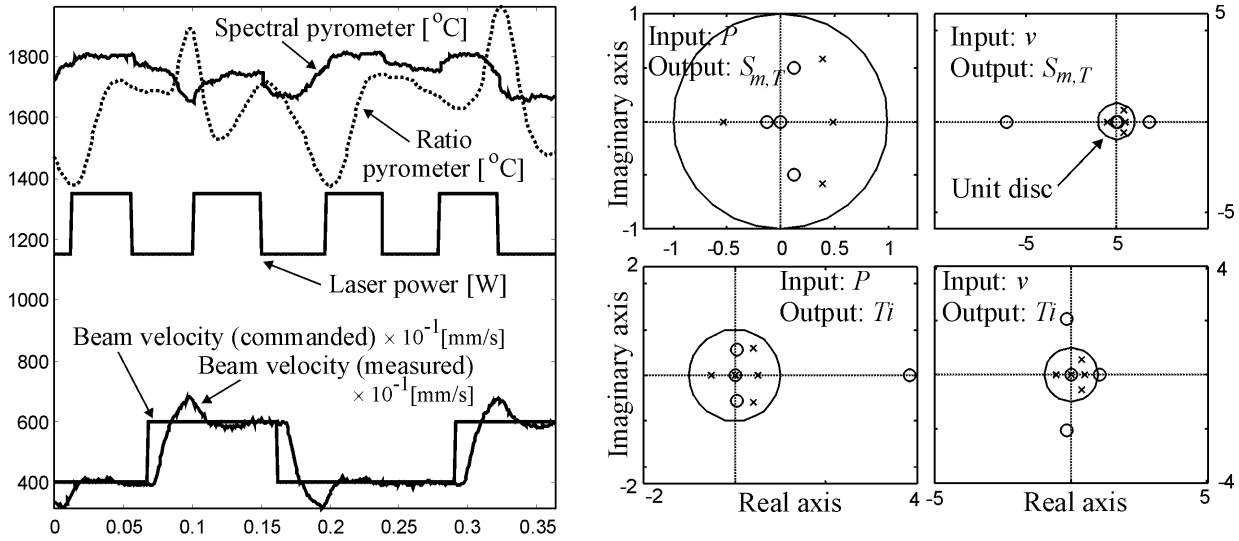

(a) Measured input and output signals

(b) Pole-Zero maps of the 4 transfer functions ×=pole, o=zero

Figure 7: Measurements and identified model

A second order (n=2, m=1 and no delays) discrete (h≈6ms) MIMO transfer function (2) was fitted[6,7]. This model proofed to be sufficiently accurate for a on-line feedback control system[6,7]. Figure 7b shows the locations of the poles and zeros of the four transfer functions (a transfer function for each input/output combination). For the models, in which the beam velocity is considered as the input, some zeros are outside the unit disc; hence this process shows NMP behavior. The zero outside the unit disc, for the model with P as input and T_i as output (lower left in figure 7b) can not be physically explained. Nevertheless, this experiment confirms the results from the theoretical model in the previous section.

4. Laser welding

In the previous sections, NMP behavior was shown for processes with the beam velocity as input. In this section, the NMP behavior of full penetration welding, using the laser power P [W] as input is shown experimentally.

A 2kW HAAS Nd:YAG laser source, equipped with a optical fiber (0.6mm core) and a lens with a focal length of 100mm was applied, see figure 8a. The focal point (0.3mm) was positioned 0.1 mm below the surface of 0.7 a mild steel plate, which was mounted on a XY-table. The experiment was a bead-on-plate weld, and was shielded with argon, both at the top as well as at backside of the plate. The light emitted by the process (plasma plume) was captured by a commercial monitoring system WELDWATCHER[9] from 4D. In this system the optical process emissions are transmitted through the fiber back to the laser source, were it is captured by an optical detector (see figure 8a). Before sampling, the detector signal is filtered by a low pass filter with a bandwidth of approximately 500Hz. The detector signal was sampled at 20kHz by a DSPACE DSP data acquisition system, hosted by a PC. This signal can be used for feedback control[10]. Also the actual laser power was sampled using this acquisition system.

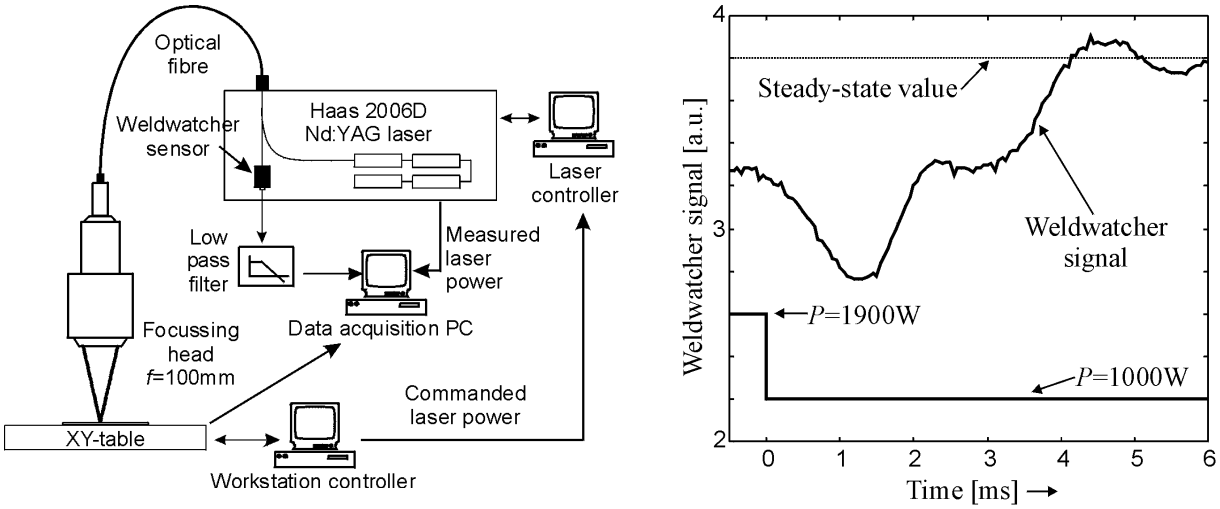

(a) Experimental setup

(b) Response of Weldwatcher sensor to a step-wise decrease of laser power.

Figure 8:Laser welding of mild steel plate

Figure 8b shows the response of the sensor to a step-wise decrease of the laser power from 1900W to 1000W at a constant welding speed of 120 mm/s. As can be observed, the signal strength decreases during the first 2ms, before increasing to its steady-state value; hence NMP behavior. It should be noted that the gain is negative-i.e. a decrease of laser power results in an increase of the signal strength.

This negative gain and the NMP behavior may be explained using figure 9. This figure shows a calculated[11] longitudinal section of the plate and the corresponding shape of the keyhole at two power levels: 1800W and 800W.

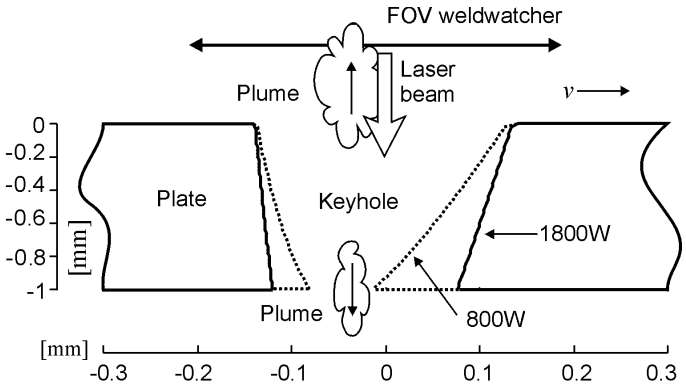

Figure 9: Longitudinal section of the plate and the calculated shape of the keyhole at 2 power levels: 1800W (solid) and 800W (dashed). v=50mm/s. The shape of the keyholes was calculated using a model of Kaplan[11].

Assume that the WELDWATCHER signal depends on the volume of plume that escapes *at the top* of the keyhole. As the keyhole is open at the bottom of the plate, also some plasma escapes at the bottom of the keyhole. Hence, the sensor signal varies when the ratio between the keyhole opening area at the top and the bottom varies. As can be observed from figure 9, if the

laser power is increased from 800 to 1800W, mainly the size of the keyhole *at the bottom* increases. Therefore, more plasma escapes from the bottom of the keyhole, resulting in a decrease of the sensor signal-i.e. a negative gain.

However, just before the keyhole opening area at the bottom is increased, an excess of material (mainly at the front of the keyhole) must be evaporated first. This results in a temporary increase of the plume at the top of the keyhole. This is probably the physical explanation of the NMP behavior during laser welding, when considering the laser power as the input of the process and the signal from the WELDWATCHER at the top. This will be subject of future work.

5. Conclusions

This paper showed theoretically as well as experimentally that laser-material processing may show nonminimum phase behavior. The NMP behavior can be explained from the difference between the beam velocity and the speed of heat diffusion into the material, during laser heating and alloying; and due to a temporary increase of the plume at the top of the product during full penetration laser welding.

Generally minimum phase systems are easier to control as their inverse transfer function $H^{-1}(s)$ is stable–i.e. no poles with positive real parts (or outside the unit disc in the case of discrete models). Stable inverses are important in control system design methods which are aimed at canceling the dynamic behavior of the process (by including the inverse transfer function $H^{-1}(s)$ in the controller) and replacing it by a desired dynamic behavior. Moreover, the NMP property of a process limits the possible attainable closed loop bandwidth.

References

[1] G.F. Franklin, J.D. Powell and A. Emami-Naeini. *Feedback control of dynamic systems*. Addison-Wesely, USA, 1986

[2] K.J. Åström and B. Wittenmark *Computer controlled systems*. 3rd edition. Prentince Hall, U.S.A., 1997.

[3] ANSYS, Inc. Southpointe, 275 Technology Drive, Canonsburg, PA 15317, U.S.A.

[4] D. Rosenthal. The theory of moving sources of heat and its application to metal treatments. *Transactions of the ASME*, **46**, pp. 849-866, 1946.

[5] A. Zambon et. al. Gas surface alloying of Ti6Al4V alloy by laser. *Proceedings of the NATO advanced study institute on laser processing*, Sesimbra, Portugal, july 3-16, pp. 327-335, 1994.

[6] G.R.B.E. Römer. *Modelling and control of laser surface treatment*. PhD-thesis, University of Enschede, the Netherlands, 1999.

[7] G.R.B.E. Römer, J. Meijer and R.G.K.M. Aarts. Multivariable control of laser alloying of Ti6Al4V. *Proceedings of the ICALEO'99*, San Diego, U.S.A., November 15-18, pp. 43-52, 1999.

[8] L. Ljung, *User's guide system identification toolbox for use with MATLAB*. The Mathworks Inc., Natick, U.S.A., 1995.

[9] Güttler, R. Sensor detects faults in keyhole. *Opto & Laser Europe*, October, pp. 13, 1998.

[10] S. Postma, R.G.K.M. Aarts, J. Meijer, J.B. Jonker, and W.M. Zweers. Penetration control in laser welding of sheet metal using optical sensors, *Proceedings of the ICALEO'2001*, Jacksonville, Florida, U.S.A., October 15-18, 2001.

[11] A. Kaplan. A model of deep penetration laser welding based on calculation of the keyhole profile. *Journal of Physics D: Applied Physics*, **27**, pp. 1805-1814, 1994.

Meet the authors

Gert-Willem Römer obtained his PhD degree in the field of modelling and control of laser surface treatment, in June 1999 at the University of Twente in the Netherlands. His current work at the chair of applied Laser Technology is addressed to seam tracking and process control for robotic laser welding.

Sjoerd Postma is a PhD-student at the Netherlands Institute for Metals Research (NIMR), in the Netherlands. His work is addressed to the development of an on-line feedback control system for laser welding, such that penetration depth is maintained during welding, despite disturbances.

Prof. Johan Meijer is head of the chair of Applied Laser Technology at the University of Twente in the Netherlands.

Niek Weerkamp is a master's student, working on FEM modelling of laser welding, at the University of Twente in the Netherlands.